

<https://doi.org/10.33472/AFJBS.6.5.2024.911-932>



African Journal of Biological Sciences



Enhancing Oxidative Performance of EMA–Na–Polyethylene–Starch Composites with Metal Oxides

Zeena P. Hamza^{1*}, Anna Dilfi K. F.², Thomas Kurian³

¹Postgraduate and Research Department of Chemistry, Maharaja's College, Ernakulam, Kerala, India, 682011

²Department of Chemistry, St. Xavier's College for Women, Aluva, Kerala, India, 683101

³Department of Polymer Science and Rubber Technology, Cochin University of Science and Technology, Kochi, Kerala, India, 682022

*Emails: zeenaphamza@maharajas.ac.in, zeenaphamza@gmail.com

***Corresponding author:** Zeena P. Hamza

* Postgraduate and Research Department of Chemistry, Maharaja's College, Ernakulam, Kerala, India, 682011

Volume 6, Issue 4, 2024
Received: 09 March 2024
Accepted: 10 April 2024
doi:10.33472/AFJBS.6.4.2024.911-932

Abstract

Metal oxides (iron oxide, manganese dioxide, titanium dioxide (anatase and rutile grades) in various compositions (0.5 and 1 weight%) were added to poly(ethylene-co-methacrylic acid) ionized with sodium cation (EMA–Na 5%) compatibilized low density polyethylene–starch blends. Mechanical properties, melt flow indices, biodegradability, photodegradability, photobiodegradability, water absorption, infrared spectroscopy, dynamic mechanical analysis, thermogravimetry, differential scanning calorimetry, and scanning electron microscopy were used to assess the role of small amounts of metal oxides as pro-oxidants in the blends. With the addition of metal oxides, the mechanical characteristics of the mixes changed. Thermal characterization using TGA and DSC revealed that the addition of metal oxides changed the thermal stability and crystallinity. Various degradative studies suggest that the inclusion of metal oxides improves the degradability of blends.

Keywords: pro-oxidant, ionomer, metal oxide, biodegradability, photodegradability, photobiodegradability

Introduction

Plastics have played a vibrant role in our day-to-day life. Synthetic plastics have mainly substituted conventional materials like paper, glass, steel, and aluminum in numerous applications over the last few decades. Plastics utilization is growing at 5% annual pace worldwide, with 227 million tons. Synthetic plastics are created to be long-lasting, resistant to various types of degradation and they have properties that other materials do not have. Plastics have an enormous role in the production of renewable energy, in reducing climate change, as well as the pharmaceutical industry, the surgical implant and assist sectors. The face mask, which is made of plastic, is currently the most sought-after commodity on the planet. Instead of banning them, should sensibly apply them where they are required to enhance the quality of life, avoid a climate disaster and, if possible, stop the spread of

infectious diseases like the corona virus (Czigány and Ronkay (2020). Many researchers are interested in learning more about low-density polyethylene (LDPE)–biodegradable formulations (Burelo, 2023; Zhang et al., 2022; Sanniyasi, 2021). Several synthetic materials, such as polyolefins, are not tarnished by environmental microorganisms, contributing to their lengthy life spans of hundreds of years. In certain conditions, Low Density Polythene is more vulnerable to microorganism outbreak than other polyolefins (Ohtake et al., 1995).

Due to environmental problems of using synthetic polymers, the application of renewable sources to fabricate packaging systems has attracted the attention of the researchers in recent years (Jiang et al., 2020, Nofar et al., 2019). The accumulation of natural polymers, such as starch, to ensure at minimum partial biodegradation is one of the feasible alternatives for speeding up the attack of microorganisms on LDPE. Starch is a good option since it is a cheap and readily available raw material (Inceoglu and Menciloglu 2013, Oner et al., 2019]. Since starch degrades at a faster pace than polyethylene, the rationale after the inclusion of biopolymer in Low Density Polythene for an enough amount of component is present in biodegradable, and if this is extracted by microorganism in the excess removal system, the base sluggish plastic can gradually fragment and vanish. The integration of polyethylene starch composites in the agricultural and biological fields represents a significant advancement in the pursuit of sustainable and eco-friendly materials. These polyethylene starch composites are particularly valuable in agriculture, where they can be utilized in applications such as mulch films, controlled-release fertilizers, and biodegradable packaging. These applications contribute to reducing plastic waste and improving soil health, ultimately promoting more sustainable agricultural practices. In the biological field, these composites offer potential in medical applications, such as biodegradable implants and drug delivery systems, due to their biocompatibility and controlled degradation properties. Starch concentrations of up to 9% for compounds and 30% for blends cause low adhesion between the phases. Modified starch has been utilized in place of native starch to enhance the LDPE–starch inter facial adhesion to enable commercial implement of these compounds (Nakamura et al., 2005; Steinmetz et al., 2016; Vinhas et al., 2007).

However, due to incompatibility between LDPE and starch, the necessary mechanical properties for packaging applications have yet to be attained (Jose et al., 2004, Ju et al., 2020, Rhim et al., 2013). Several patents have been filed on the utilization of ionomers as compatibilizers in polymer blends (Mural et al., 2014). Zn and Na salts of polyethylene–co–methacrylic acid ionomers have also been investigated as compatibilizers for LDPE–starch blends (Gemeinhardt et al., 2004). The addition of ionomers enhanced the mechanical properties of the blends, representative that ionomers are efficient compatibilizers for LDPE–starch blends and that the inclusion of ionomers has little impact on the blend's biodegradation. An ionomer is a polymer chain with a minor fraction of ion-containing monomer units, taken in the state of which counter ions are not permitted, but condensed on the corresponding co-ions of the polymer chains and forming ion pairs, as described by various authors (Zhang et al., 2014, Peter et al., 2014, Guo and Wang 2019).

This is not an easy task to destroy recycled plastics in the field. Plastic degradation under thrilling conditions, like burning, is not an easy fleshly process. Photo-oxidation of LDPE–starch blends covering pro-oxidants causes chain scission, resulting in a rise of the low molecular weight fraction, which encourage biodegradation (Ammala et al., 2011, Deepika and Jaya 2015, Jakubowicz, 2016). Pro-oxidants are the substances that encourage oxidative pressure by generating reactive oxygen species (Bardaji, 2020, Oromiehie, 2013). Photo-oxidation of the blends containing pro-oxidants increase the low molecular weight segments by chain scission, thereby enabling biodegradation (Menofy and Khattab 2022, Mahieu, 2015, Sabetzadeh, 2016). It also increases the surface area through embrittlement and subsequent track formation. In addition, the formation of carbonyl groups

on the surface increases the hydrophilicity of polyethylene. It is reported that transition metals, especially iron and manganese, can act as effective photo initiators for polyethylene by decomposing the hydroperoxides formed during its oxidation (Wilpiszewska and Szychaj 2011, Queiroz and Collares-Queiroz 2020, Kfoury et al., 2013). Use of TiO₂ as photocatalyst is also reported owing to its excellent characteristics such as high photo activeness, stability, non-toxicity and inexpensiveness (Watanabe 2010, Arkatkar 2009).

This study investigates the use of metal oxides, specifically ferric oxide, manganese dioxide, and titanium dioxide (anatase and rutile grades), to improve the degradative qualities of poly(ethyleneco-methacrylic acid) ionized with sodium cation compatibilized low density polyethylene-starch blends. The use of these composites exemplifies a strategic approach to addressing environmental concerns while maintaining functionality and efficiency in agricultural and biological applications. Table 1 shows the sample designations and descriptions utilized in this work. Mechanical properties, infrared spectroscopy, thermal properties, and scanning electron microscopy were used to characterize the films. The films' biodegradability, photodegradability, and photobiodegradability were also tested.

Table 1. Description of sample designations

Sample designation	Description
LDS-Na	LDPE-20% starch-5% (EMA-Na)
LDS-Na-Fe	LDPE-20% starch-5% (EMA-Na)-Fe ₂ O ₃
LDS-Na-Mn	LDPE-20% starch-5% (EMA-Na)-MnO ₂
LDS-Na-Ru	LDPE-20% starch-5% (EMA-Na)-TiO ₂ (rutile)
LDS-Na-An	LDPE-20% starch-5% (EMA-Na)- TiO ₂ (anatase)

Materials and methods

Materials:

Low density polyethylene (LDPE)

The film grade low density polyethylene (LDPE 24FS040) from Reliance Industries Limited, Mumbai, India, with melt flow index (190 °C/2.16 kg) of 4 g/10 min and density (23 °C) of 0.922 g/cm³ was supplied by Periyar Polyfilms, Edayar, Kerala, India.

Starch

The tapioca starch (100 and 300 mesh) was obtained from Jemsons Starch & Derivatives, Aroor, Alappuzha, Kerala. As these fillers were hygroscopic in nature they were oven dried at 120 °C for 1h prior to mixing.

Ionomers

Ionomer used in this study was sodium salt of poly(ethylene-co-methacrylic acid) (HIMILAN 1555 EMAANa) with melt flow index (190°C/2.16 kg) of 10 g/10 min. These ionomers were supplied by Mitsubishi Plastics, Inc., Japan.

Pro-oxidants

Metal oxides such as iron oxide, manganese dioxide, and titanium dioxide (anatase and rutile grades) were used as pro-oxidants in this study. Merck Specialities Pvt. Ltd., Mumbai, India, supplied the

iron oxide. Qualigens Fine Chemicals, Mumbai, India, supplied the manganese dioxide. Associated Chemicals, Edappally, Kerala, India, supplied titanium dioxide (anatase and rutile grades).

Methods:

Preparation of blends

A Thermo Haake Polylab system (Rheocord 600p) equipped with roller-type rotors was used for melt mixing. The mixing chamber has a volumetric capacity of 69 cm³. A mixing time of 8 minutes was given for all the compounds at a rotor speed of 30 rpm at 150 °C. LDPE together with ionomer was first melted for 2 minutes followed by the addition of filler. Mixing was continued for another 6 minutes.

Preparation of test specimens

The test specimens were prepared from neat LDPE and the compounds by moulding in an electrically heated hydraulic press for 5 minutes at 150°C under a pressure of 20 MPa. After moulding, the samples were cooled down to room temperature under pressure.

Characterization:

Mechanical properties

The mechanical properties were evaluated using Shimadzu Autograph AG-I series universal testing machine at a crosshead speed of 50 mm/min. Tensile strength, elongation at break and elastic modulus were measured according to ASTM D-882 (2002). Averages of at least five sample measurements were taken to represent each data point.

Melt Flow Index (MFI)

The melt flow index (MFI) of each blend of LDPE with filler was measured using a CEAST Modular Line Melt Flow Indexer in accordance with ASTM method D-1238 using a 2.16 kg load at a melt temperature of 190°C.

Biodegradation studies

The biodegradation studies on the blends were carried out according to ASTM D-6691. Bacterial cultures were obtained from culture collections of Microbial Genetic Lab, Department of Biotechnology, Cochin University of Science and Technology. These cultures were isolated from sediment samples collected from different locations in Cochin backwaters and Mangalavanam mangroves. These cultures were previously identified as the genus *Vibrionacea* based on their morphological and biochemical characteristics outlined in Bergey's Manual of Systematic Bacteriology (Rosa et al., 2009). They were preserved in 10mL glass bottles employing the paraffin oil overlay method.

To prepare the inoculum the individual isolates of the consortium were grown overnight at 37°C at 120 rpm on an Orbitek shaker (Scigenics Pvt. Ltd, Chennai, India) in nutrient broth (Himedia, Mumbai) pH 7.0 ± 0.3 with 1% NaCl. The cells were harvested by centrifugation at 5000 rpm (2292 g) for 20 minutes, washed with physiological saline and then pooled. 5mL of this pooled culture (OD₆₆₀ = 1) was used to inoculate 50mL amylase minimal medium (Roy et al 2009) lacking starch. The samples prepared from the blends previously wiped with 70% alcohol were added to this medium and these strips acted as the sole source of carbon. Incubation was in the Orbitek environmental shaker at 37 °C and 120 rpm for a total period of 3 months with regular sampling. The medium without the

inoculum with corresponding starch–plastic blends and subjected to the same treatment as above were used as controls.

Soil burial test

The soil burial test was also carried out to evaluate the biodegradability of the blends. The soil was taken into pots and the plastic strips were placed in it. The bacterial culture was supplied to the soil. Care was taken to ensure that the samples were completely covered with soil. The pot was then kept at room temperature. The loss in weight and tensile strength was measured after thorough washing with water and drying in an oven until constant weight to determine the extent of biodegradability.

Photodegradation by UV rays

In the present study, the plastic film samples were cut to 8x1 cm size and exposed under a 30watt shortwave UV lamp at a distance of 30 cm. The plastic films were then taken out after one month to determine tensile strength using a universal testing machine. Average weight of the test specimens, before and after the degradation studies were carried out using a Sartorius–0.1 mg electronic balance. The FTIR and DSC were used for the characterization and monitoring of the functional group changes in the samples during irradiation.

Water absorption characteristics

Water absorption was measured using 3 x 1 inch film strips of <1mm thickness according to ASTM D–570–81 method. Water absorption measurements were performed by soaking the samples in distilled water. The water absorption was calculated as the weight difference and is reported as a percentage increase of the initial weight. The results reported are average of three measurements.

Fourier transform infrared spectroscopy (FTIR)

The FTIR spectra of the samples were recorded in the transmittance mode using a Thermo Nicolet, Avatar 370 FTIR spectrophotometer in the spectral range of 4000–400 cm^{-1} .

Dynamic mechanical analysis (DMA)

Dynamic Mechanical Analyzer (DMA Q–800, TA instruments) was used to study the viscoelastic properties of the samples. DMA analysis was conducted at a constant frequency of 1 Hz. A temperature ramp was run from 40 °C to 100 °C to get an overview of the thermomechanical behaviour of the samples. The dynamic storage modulus, loss modulus and $\tan \delta$ were measured.

Thermogravimetric analysis (TGA)

Thermogravimetric analysis was carried out in a TGA Q–50 thermal analyzer (TA Instruments) under a nitrogen atmosphere. The samples were heated from room temperature to 600 °C at a heating rate of 20 °C/min and a nitrogen gas flow rate of 40–50 cm^3/min . The sample weights varied from 10–15 mg. The weight changes were noted with the help of an ultra sensitive microbalance. The data of weight loss versus temperature and time were recorded online using the TA Instrument's Q Series Explorer software. The analysis of the thermogravimetric (TG) and derivative thermogravimetric (DTG) curves was done using TA Instrument's Universal Analysis 2000 software version 3.3 B. The temperature at which weight loss is maximum (T_{max}) was evaluated.

Differential scanning calorimetry (DSC)

The crystallinity of the samples was studied using a TA Q-100 thermal analyzer (TA Instruments) under nitrogen atmosphere with a heating rate of 10 °C/min. Samples of 5–10 mg were heated in a nitrogen atmosphere from –50°C to 150°C and kept at 150°C for 3 min to erase the thermal history. Then a cooling was performed from 150°C to –50 °C, followed by a second heating from –50°C to 150°C at the same rate. The percentage of crystallinity was calculated from the DSC traces as follows.

$$\% \text{ Crystallinity} = (\Delta H_{f(\text{obs})} / \Delta H_{f(100\% \text{ crystalline})}) \times 100$$

where $\Delta H_{f(\text{obs})}$ is the enthalpy associated with melting of the material and $\Delta H_{f(100\% \text{ crystalline})}$ is the enthalpy of 100% crystalline polyethylene reported in the literature to be 286.7J/g.

Morphological studies

In the present study the tensile fractured surfaces were mounted on a metallic stub with the help of a silver tape and conducting paint in the upright position and were sputter coated with platinum within 24 hours of fractures in a JFC 1600 Autofine coater and then examined under JEOL model JSM-6390LV scanning electron microscope (SEM).

Results and Discussion

Mechanical properties

Figure 1 illustrates the mechanical properties of pure LDPE, LDPE–starch–(EMA–Na) blend, and blends incorporating metal oxides as pro-oxidants.

One key mechanical parameter assessed is the tensile strength of these materials, which denotes the maximum stress a material can withstand when subjected to pulling forces without fracturing. Notably, the figures reveal that the samples containing metal oxides exhibit tensile strength values within a comparable range to that of the pristine LDPE. This suggests that the incorporation of metal oxides, which serve as pro-oxidants, has not led to a noteworthy decline in tensile strength. This is significant because it indicates that the processing techniques and the presence of metal oxides have not induced premature degradation reactions within the materials (Ferreira 2009).

However, in terms of elongation at break, a different trend emerges. The materials with metal oxide additives exhibit a notable reduction in elongation at break compared to the pristine LDPE. This suggests that the incorporation of metal oxides impairs the material's ability to stretch before fracture. This finding could be associated with changes in the material's structure, such as increased crosslinking or alterations in polymer chain mobility, due to the presence of metal oxides.

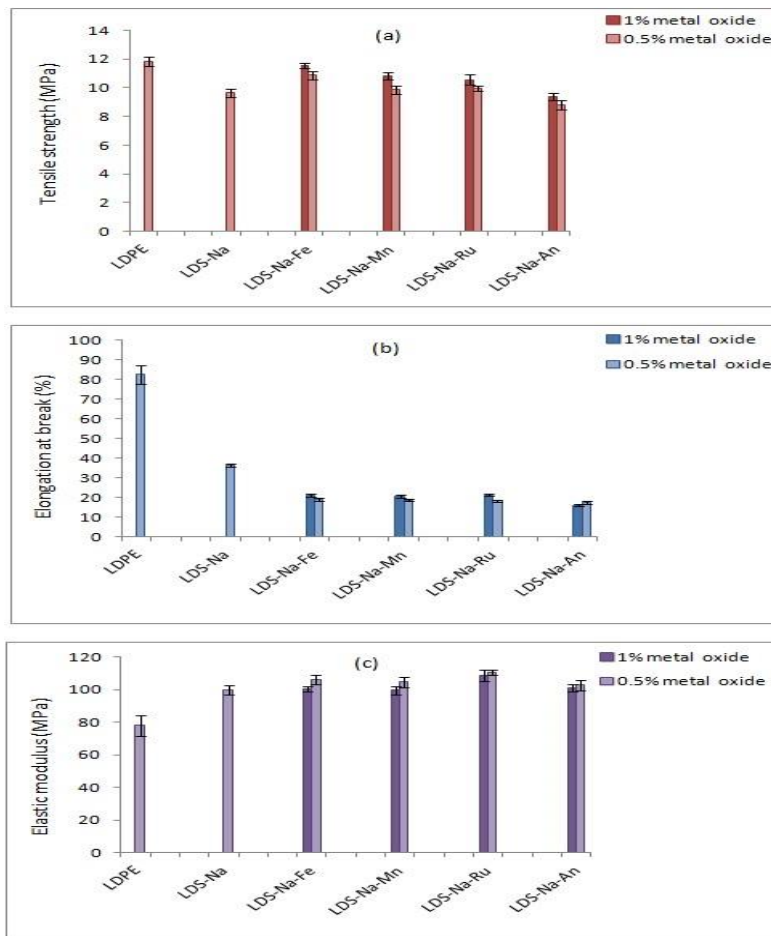


Figure 1. Effect of metal oxides on the mechanical properties of LDPE-starch-(EMA-Na) blends

Additionally, Figure 1(c) shows an increase in the elastic modulus of the blends containing metal oxides. The elastic modulus represents a material's stiffness and resistance to deformation under an applied load. In this context, the results indicate that all blend compositions, including those with metal oxides, possess higher elastic moduli than pure LDPE. This points to an increase in stiffness across the blends (Burjupati 2020).

Melt flow measurements

Figure 2 shows the effect of metal oxides on the melt flow indices of LDPE-starch-(EMA-Na) blends. The melt flow index (MFI) is a measure of a polymer's flowability under heat and pressure, indicating how easily it can be processed. A higher MFI indicates a greater ability to flow. Conversely, a lower MFI implies higher viscosity and reduced flowability.

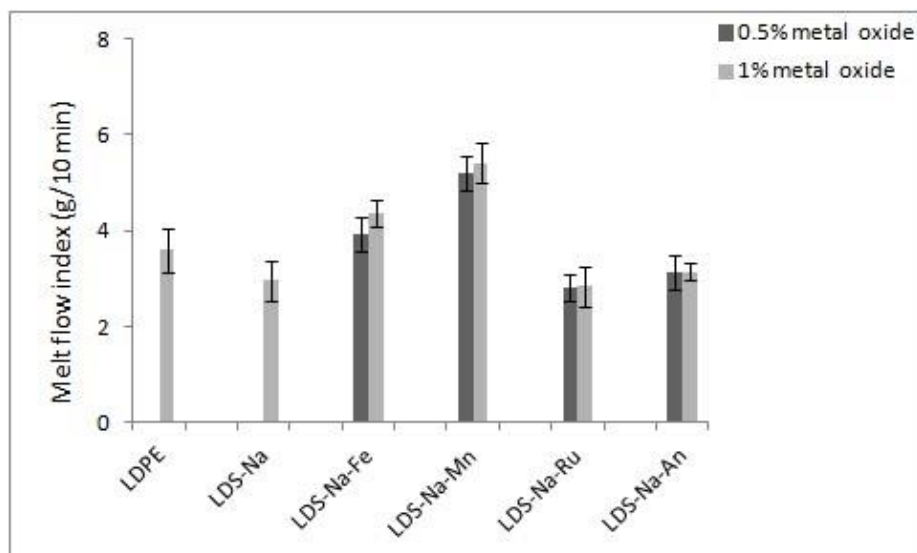


Figure 2. Effect of metal oxides on the melt flow indices of LDPE–starch–(EMA–Na) blends

For most samples of LDPE–starch–(EMA–Na) blends containing metal oxides, the MFI values are quite similar to the MFI of pure LDPE. This observation suggests that the inclusion of these metal oxides as pro-oxidants during processing does not lead to significant chain scission (breaking of polymer chains) or crosslinking (joining of polymer chains) that would cause a substantial change in the melt flow indices. This is indicative of a controlled processing environment where the prooxidants do not induce major structural changes in the polymer matrix.

The exception to this trend is found with Fe_2O_3 (iron oxide) and MnO_2 (manganese dioxide) additives. In LDPE–starch–(EMA–Na) blends incorporating Fe_2O_3 and MnO_2 , the MFI values increase significantly. This increase signifies notable chain scission occurring within the polymer chains. Chain scission often results in a decrease in molecular weight, leading to a higher flowability under heat.

This variation in behaviour could be attributed to the specific interactions between the metal oxides and the polymer matrix. Different metal oxides may catalyse reactions to differing extents, leading to distinct levels of chain scission or crosslinking. Reference (Kushwaha 2023) likely offers further insights into the underlying mechanisms driving these observations, possibly discussing the chemical and physical interactions between metal oxides and the polymer blend constituents.

Biodegradation studies

Figure 3 presents the tensile characteristics of LDPE–starch–(EMA–Na)–metal oxide blends. These blends underwent a two-month biodegradation process within a culture medium. Additionally, Table 2 provides information about the percentage decrease in tensile strength observed in these blends.

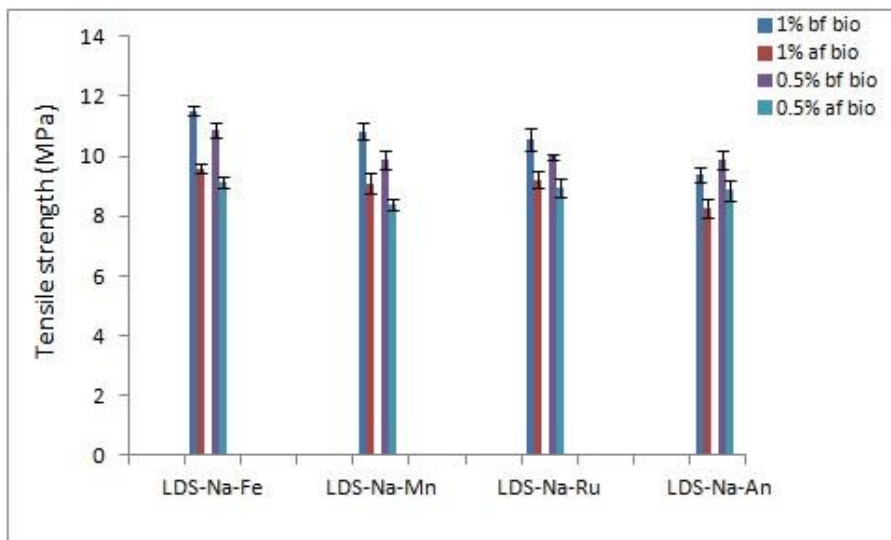


Figure 3. Biodegradation of LDPE–starch–(EMA–Na)–metal oxide blends after immersion of plastic strips in culture medium for two months (Evident from tensile strength)

Table 2. Percentage decrease in tensile strength of LDPE–starch–(EMA–Na)–metal oxide blends after biodegradation in culture medium for two months

Sample	Initial tensile strength (MPa)	Tensile strength after biodegradation for two months (MPa)	% decrease in tensile strength
LDS–Na(1)Fe	11.5 + 0.17	9.59 + 0.15	16.79
LDS–Na(0.5)Fe	10.9 + 0.26	9.15 + 0.18	15.77
LDS–Na(1)Mn	10.8 + 0.26	9.10 + 0.32	16.05
LDS–Na(0.5)Mn	9.86 + 0.31	8.37 + 0.18	15.09
LDS–Na(1)Ru	10.6 + 0.35	9.21 + 0.29	12.87
LDS–Na(0.5)Ru	9.99 + 0.08	8.95 + 0.33	10.39
LDS–Na(1)An	9.38 + 0.23	8.24 + 0.31	12.11
LDS–Na(0.5)An	9.91 + 0.31	8.86 + 0.37	10.57

The biodegradation process led to a significant reduction in the tensile strength of the blends (Maziad 2021). This outcome is evident from the figure, which visually depicts the change in tensile properties after the biodegradation period. The main factor driving this reduction is the microbial consumption of starch present in the blends. The interaction between microbes and the starch component results in its degradation, leading to a weakening of the overall structure and subsequently causing a decline in tensile strength. The information from Table 2 offers a quantitative perspective on the extent of tensile strength decrease for the blends following biodegradation. These data add a more precise measurement to the understanding of how the blends' mechanical properties were affected. Moreover, weight loss is highlighted as a crucial factor in assessing the biodegradation of polymers. Table 3 consolidate information on the percentage weight loss experienced by the blends after the biodegradation process in the culture medium. The results underscore the extent of degradation that

occurred during the biodegradation period. The considerable weight loss across all samples after exposure to the culture medium indicates that the LDPE–starch–(EMA–Na) blends containing metal oxides are indeed partially biodegradable.

Table 3. Percentage decrease in weight of LDPE–starch–(EMA–Na)–metal oxide blends after biodegradation in culture medium for two months

Sample	Initial weight (g)	Weight after two months (g)	% weight loss
LDS–Na(1)Fe	0.4633	0.4510	2.669
LDS–Na(0.5)Fe	0.6113	0.5957	2.552
LDS–Na(1)Mn	0.4724	0.4598	2.674
LDS–Na(0.5)Mn	0.5065	0.4944	2.398
LDS–Na(1)Ru	0.5544	0.5404	2.534
LDS–Na(0.5)Ru	0.6442	0.6295	2.283
LDS–Na(1)An	0.4953	0.4870	1.674
LDS–Na(0.5)An	0.4335	0.4268	1.559

Photodegradation studies

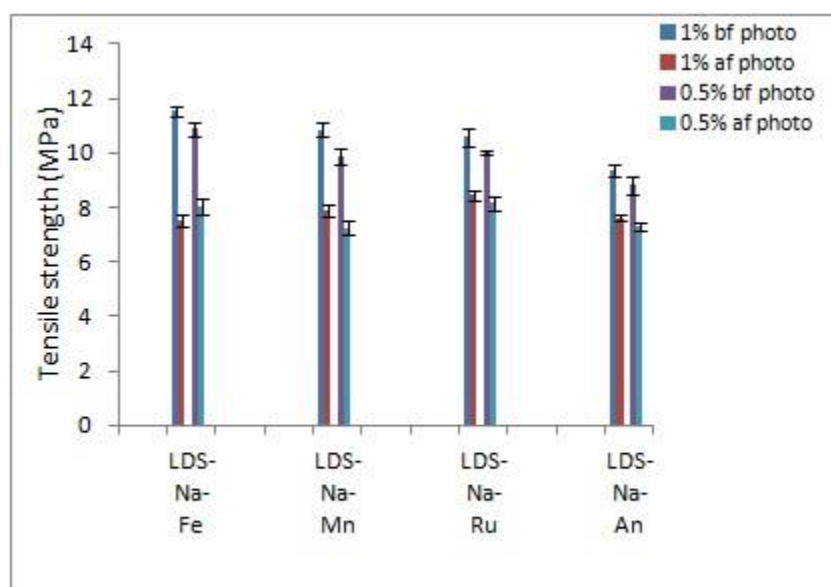


Figure 4. Photodegradation of LDPE–starch–(EMA–Na)–metal oxide blends after UV exposure for one month (Evident from tensile strength)

Figure 4 within the study depict the tensile characteristics of LDPE–starch–(EMA–Na)–metal oxide blends, following one month of exposure to ultraviolet (UV) light. Complementing this figure, Table 4 provide specific information about the percentage decrease in tensile strength of blends due to the UV exposure.

Table 4. Percentage decrease in tensile strength of LDPE–starch–(EMA–Na)–metal oxide blends after UV exposure for one month

Sample	Initial tensile strength (MPa)	Tensile strength (MPa) after UV exposure for one month	% decrease in tensile strength
LDS–Na(1)Fe	11.5 + 0.17	7.52 + + 0.25	34.61
LDS–Na(0.5)Fe	10.9 + 0.26	8.02 + 0.30	26.17
LDS–Na(1)Mn	10.8 + 0.26	7.86 + 0.23	27.49
LDS–Na((0.5)Mn	9.86 + 0.31	7.34 + 0.28	25.54
LDS–Na(1)Ru	10.6 + 0.35	8.45 + 0.19	20.06
LDS–Na(0.5)Ru	9.99 + 0.08	8.15 + 0.28	18.40
LDS–Na(1)An	9.38 + 0.23	7.61 + 0.12	18.83
LDS–Na(0.5)An	8.81 + 0.31	7.27 + 0.15	17.45

A clear pattern emerges from the figure and table, as the tensile strength of the blends undergoes a significant reduction after one month of UV light exposure. This effect is supported by the quantified data provided in the table, revealing the extent of tensile strength decrease.

The UV exposure leads to changes in the chemical structure of the blends. Specifically, the polymer chains undergo modifications, resulting in the creation of new functional groups within the polymer structure. This phenomenon is particularly prominent in the amorphous regions of the material. The introduction of these new groups can influence the mechanical properties of the blends. In this case, the observed decrease in tensile strength can be attributed to these chemical changes induced by the UV exposure (Bulatovic 2021).

Furthermore, Table 5 provides insight into the weight loss experienced by the LDPE–starch–(EMANA)–metal oxide blends following one month of UV exposure. The data reveal that all the samples undergo a slight decrease in weight after photodegradation. Moreover, the weight loss is found to increase as the concentration of metal oxides in the blends increases. This information suggests that the presence of metal oxides could influence the susceptibility of the blends to UV–induced degradation.

Table 5. Percentage decrease in weight of LDPE–starch–(EMA–Na)–metal oxide blends after UV exposure for one month

Sample	Initial weight (g)	Weight(g) after month	% weight loss
LDS–Na(1)Fe	0.5950	0.5930	0.336
LDS–Na(0.5)Fe	0.5333	0.5326	0.244
LDS–Na(1)Mn	0.4634	0.4621	0.281
LDS–Na(0.5)Mn	0.4785	0.4774	0.230
LDS–Na(1)Ru	0.6540	0.6527	0.199
LDS–Na(0.5)Ru	0.4408	0.4403	0.113
LDS–Na(1)An	0.6010	0.5999	0.183
LDS–Na(0.5)An	0.5495	0.5489	0.109

Photobiodegradation studies

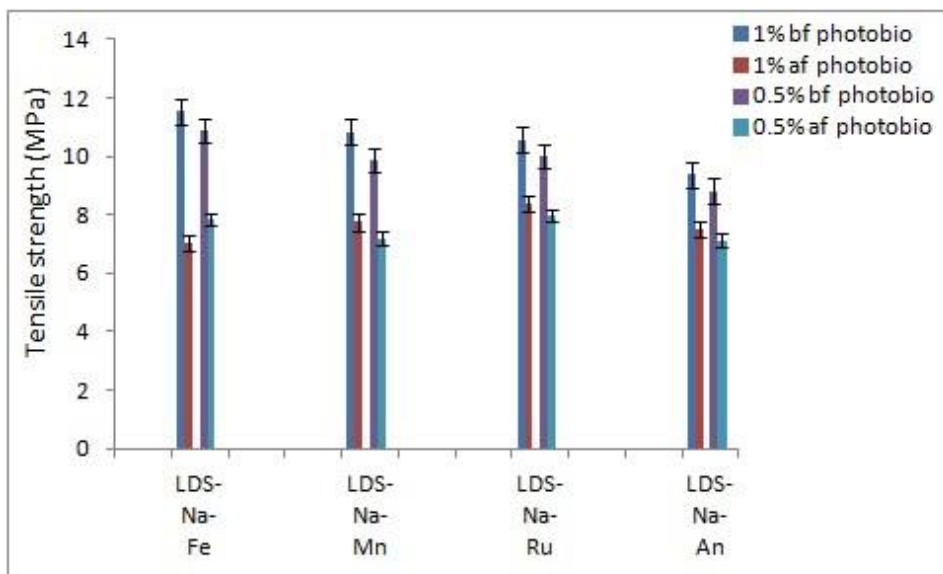


Figure 5. Variation in tensile strength of LDPE–starch–(EMA–Na)–metal oxide blends after UV exposure for one month followed by biodegradation in culture medium for one month

Figure 5 showcase the tensile properties of LDPE–starch–(EMA–Na)–metal oxide blends. These blends underwent photobiodegradation experiments, involving a two–step process: exposure to UV light for one month, followed by immersion in culture media containing amylase–generating vibrios isolated from the marine benthic environment for an additional month. Table 6 provides details about the percentage decrease in tensile strength for each blend type after the photobiodegradation process. The results in Figure 5 highlight a substantial reduction in the tensile strength of both types of blends following two months of photobiodegradation. The data from Table 6 quantify this reduction in tensile strength, further underscoring the extent of the change.

Table 6. Percentage decrease in tensile strength of LDPE–starch–(EMA–Na)–metal oxide blends after photobiodegradation

Sample	Initial tensile strength (MPa)	Tensile strength(MPa) after photobiodegradation for two months	% decrease in tensile strength
LDS–Na(1)Fe	11.5 + 0.17	7.01 + 0.15	39.04
LDS–Na(0.5)Fe	10.9 + 0.26	7.83 + 0.11	28.17
LDS–Na(1)Mn	10.8 + 0.26	7.75 + 0.16	28.24
LDS–Na((0.5)Mn	9.86 + 0.31	7.18 + 0.10	27.17
LDS–Na(1)Ru	10.6 + 0.35	8.37 + 0.18	21.11
LDS–Na(0.5)Ru	9.99 + 0.08	7.98 + 0.11	20.10
LDS–Na(1)An	9.38 + 0.23	7.49 + 0.16	20.11
LDS–Na(0.5)An	8.81 + 0.31	7.12 + 0.12	19.16

The photobiodegradation process involves a synergy between UV exposure and microbial activity. The exposure to UV light initiates a photo–oxidation process within the pro–oxidant–containing polyethylene–starch–ionomer blends. This process leads to the formation of oxidation products and

an increase in the low molecular weight fraction due to chain scission. As a result, the blends become more susceptible to biodegradation (Rosa et al., 2009).

Table 7. Percentage decrease in weight of LDPE–starch–(EMA–Na)–metal oxide blends after photobiodegradation for two months

Sample	Initial weight (g)	Weight after two months (g)	% weight loss
LDS–Na(1)Fe	0.5950	0.5867	1.395
LDS–Na(0.5)Fe	0.5333	0.5272	1.144
LDS–Na(1)Mn	0.4634	0.4575	1.273
LDS–Na(0.5)Mn	0.4785	0.4725	1.254
LDS–Na(1)Ru	0.6010	0.5943	1.115
LDS–Na(0.5)Ru	0.5495	0.5436	1.074
LDS–Na(1)An	0.6540	0.6468	1.101
LDS–Na(0.5)An	0.4408	0.4361	1.066

Additionally, Table 7 detail the percentage weight loss observed in the blends after undergoing biodegradation in the culture medium. Following photobiodegradation, all samples experience a significant loss in weight. This weight loss is attributed to the microbial breakdown of the oxidation products formed during the photobiodegradation process. Microbes utilize these oxidation products as a substrate, leading to the observed weight loss.

Water absorption studies

Percentage water absorption tests were conducted to assess the hydrophilicity level of LDPEstarch–(EMA–Na)–metal oxide blends. In this context, Table 8 provides an overview of the water absorption characteristics exhibited by these composites. The goal of these tests is to determine the extent to which water is absorbed by the blends, indicating their propensity to interact with and absorb moisture.

Table 8. Water absorption of LDPE–starch–(EMA–Na)–metal oxide blends

Sample	Initial weight (g)	Weight (g) after 24 hours	% water absorption
LDS–Na(1)Fe	0.3912	0.3960	1.227
LDS–Na(0.5)Fe	0.2691	0.2723	1.189
LDS–Na(1)Mn	0.2959	0.2994	1.183
LDS–Na(0.5)Mn	0.2884	0.2918	1.179
LDS–Na(1)Ru	0.3278	0.3315	1.129
LDS–Na(0.5)Ru	0.2427	0.2451	0.989
LDS–Na(1)An	0.3363	0.3396	0.981
LDS–Na(0.5)An	0.2913	0.2940	0.927

The data in Tables 9 reveal that the presence of metal oxides in the blends does not lead to any significant alteration in their water absorption behaviour, when compared to the blends without metal

oxides. This implies that the addition of metal oxides does not notably affect the blends' overall capacity to absorb water.

Table 9. Water absorption of LDPE–starch–(EMA–Na) blends

Sample	Initial weight (g)	Weight (g) after 24 hours	% water absorption
LDS(0)–Na(2)	0.3682	0.3684	0.05
LDS(0)–Na(5)	0.3773	0.3774	0.03
LDS(15)–Na(2)	0.3021	0.3043	0.73
LDS(15)–Na(5)	0.5418	0.5450	0.59
LDS(20)–Na(2)	0.3436	0.3480	1.28
LDS(20)–Na(5)	0.5418	0.5485	1.25
LDS(30)–Na(2)	0.4653	0.4723	1.50
LDS(30)–Na(5)	0.3344	0.3389	1.35
LDS(40)–Na(2)	0.2395	0.2473	3.26
LDS(40)–Na(5)	0.3513	0.3579	1.88

(LDS(0)–Na(2) = LDPE– 0%starch–2% EMA–Na; LDS(0)–Na(5) = LDPE– 0%starch–5% EMA–Na; LDS(15)–Na(2) = LDPE– 15%starch–2% EMA–Na; LDS(15)–Na(5)= LDPE– 15%starch–5% EMA–Na; LDS(20)–Na(2) = LDPE– 20%starch–2% EMA–Na; LDS(20)–Na(5) = LDPE– 20%starch–5% EMA–Na; LDS(30)–Na(2) = LDPE–30%starch–2% EMA–Na; LDS(30)–Na(5) = LDPE– 30%starch–5% EMA–Na; LDS(40)–Na(2) = LDPE– 40%starch–2% EMA–Na; LDS(40)–Na(5) = LDPE–40%starch–5% EMA–Na)

Additionally, the data points out a distinct trend in water absorption among the various compositions. Specifically, when considering films containing 1% metal oxides in EMA–Na compatible blends, the percentage water absorption follows a specific order: LDS–(1)Fe > LDS(1)Mn > LDS–(1)Ru > LDS–(1)An. This sequence signifies that the blend containing iron oxide (Fe) exhibits the highest water absorption rate, followed by manganese dioxide (Mn), rutile–grade titanium dioxide (Ru), and anatase–grade titanium dioxide (An). This information provides insights into how different metal oxides impact the hydrophilicity of the blends. 3.7 FTIR spectroscopy

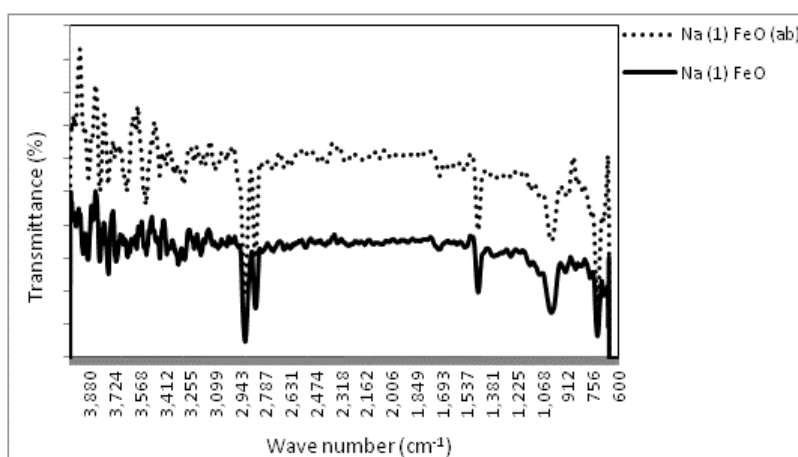


Figure 6. FTIR spectra of LDPE–starch–(EMA–Na)–1% Fe₂O₃ blend:

(–) before biodegradation and (...) after biodegradation

Figure 6 depicts the FTIR spectrum of the LDPE–starch–(EMA–Na)–Fe₂O₃ film before and after biodegradation. Table 10 shows the spectra of the LDPE–starch–(EMA–Na)–Fe₂O₃ film, which has different absorption peaks. The symmetrical stretching vibration of C–H bonds, CH₂ scissor and

asymmetric bending, and CH₂ rocking vibrations create peaks at 2912–2847 cm⁻¹, 1463 cm⁻¹, and 721 cm⁻¹.

Table 10. Characteristic FTIR spectral peaks

Sample	Peak position (cm ⁻¹)	Characteristic group
LDPE- starch- (EMA-Na)-Fe ₂ O ₃ film	2912, 2847	C-H stretching
	1537	C=O stretching
	1463	CH ₂ scissor and bending asymmetric
	1368	C-H bending
	1008	O-C stretching
	918	O-H deformation
	721	CH ₂ rocking

As shown in the figure, peak intensities of films at 2912–2847 cm⁻¹, 1463 cm⁻¹, and 721 cm⁻¹ were all significantly increased after two months of biodegradation in culture. Peak intensity has increased due to polyethylene chain fracture under degradable conditions, which has resulted in an increase in terminal group numbers. Furthermore, the carbonyl group formed during polyethylene oxidation was responsible for the peak at 1537 cm⁻¹ after breakdown. The anhydroglucose ring OC stretch is responsible for the peak at 1008 cm⁻¹. Peak intensity of starch and polyethylene also improved marginally.

It is evident that the breakdown of polyethylene under degradable conditions resulted in an increase in terminal group numbers, leading to an increase in peak intensity. Additionally, the biodegradation of LDPE-starch-(EMA-Na) blends was not negatively affected by the presence of ferric oxide.

Dynamic mechanical analysis

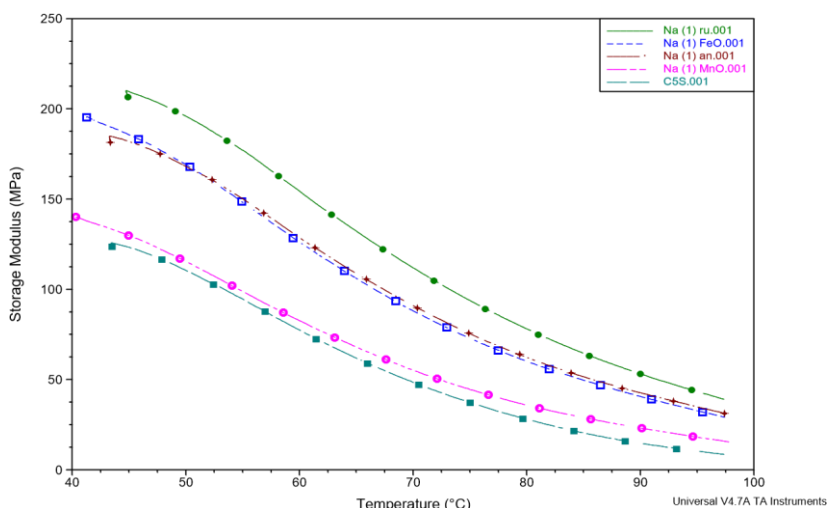


Figure 7. DMA curves of LDPE-starch-(EMA-Na)-1% metal oxide blends

Figure 7 in the study provides graphical representations of the changes in storage modulus observed in LDPE-starch-(EMA-Na) blends that incorporate metal oxides. These measurements were taken over a temperature range spanning from 40°C to 100°C. The storage modulus is a measure of a material's

ability to store and return energy under deformation, representing its stiffness or resistance to deformation.

The key observation drawn from these figures is that the presence of metal oxides in the blends led to an increase in the values of the storage modulus. This upward shift in the storage modulus values indicates an enhancement in the stiffness and rigidity of the blends. Essentially, the materials became less deformable in response to applied forces.

This change in stiffness can be attributed to an improvement in the interfacial contact between the different phases present within the blends. In polymer blends, different components often have different properties, and achieving good interfacial adhesion is essential for maintaining the integrity of the material. The introduction of metal oxides appears to have contributed to a stronger interfacial interaction, which, in turn, led to higher storage modulus values (Bulatovic 2021).

Thermogravimetric analysis (TGA)

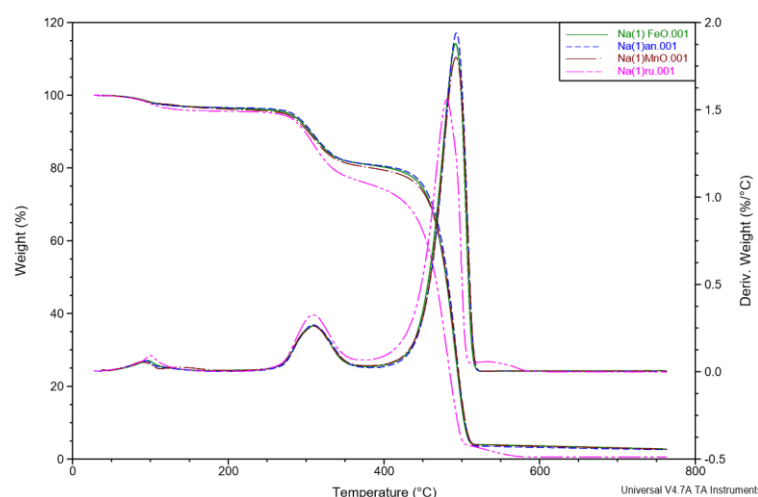


Figure 8. TGA thermograms of LDPE-starch-(EMA-Na)-1% metal oxide blends

Figure 8 within the study depict thermograms of LDPE-starch-(EMA-Na)-1% metal oxide blends. These thermograms offer insights into the thermal breakdown behavior of these blends under increasing temperature conditions (Monje, 2021).

The thermograms show distinct regions of weight loss, each corresponding to specific thermal degradation processes.

1. First weight loss region (Approximately 100°C): This initial weight loss region can be attributed to the thermal degradation of low molecular weight constituents within the blend. These are likely components with lower molecular weight and weaker bonds that undergo thermal breakdown at relatively lower temperatures.
2. Second weight loss region (225°C–350°C): The weight loss observed in this region can be linked to the thermal breakdown of starch within the blend. Starch is a polysaccharide that can degrade when exposed to elevated temperatures. The thermal degradation of starch could result in the release of volatile compounds and the reduction in the overall mass of the blend.
3. Third weight loss region (420°C–525°C): This weight loss region is attributed to the thermal degradation of the backbone chains of pure polyethylenes. The main structural components of polyethylene chains undergo thermal breakdown at these higher temperatures.

Table 11 presents summarized thermogravimetric parameters for the different blends, providing a quantitative perspective on their thermal stability. The data suggest that the presence of metal oxides

in LDPE–starch–(EMA–Na) composites leads to a reduction in their thermal stability. In other words, the blends containing metal oxides tend to degrade at lower temperatures compared to those without metal oxides.

Table 11. Results of thermogravimetric analysis of LDPE–starch–(EMA–Na)–1% metal oxide blends

Sample	Temperature of onset of degradation (°C)	T _{max} (°C)	Rate of maximum degradation (%/°C)	Residual weight (%)
LDS–Na	430.41	492.37	2.079	1.870
LDS–Na(1)Fe	423.23	491.78	1.878	2.747
LDS–Na(1)Mn	420.50	492.14	1.802	2.773
LDS–Na(1)Ru	411.48	480.41	1.558	0.5767
LDS–Na(1)An	422.82	492.75	1.940	2.577

This decrease in thermal stability could be attributed to interactions between the metal oxides and the polymer matrix. These interactions might promote degradation pathways or accelerate the breakdown of polymer chains under thermal stress. The insights provided by this information contribute to understanding how the presence of metal oxides impacts the thermal behavior of LDPE–starch–(EMA–Na) blends. This has implications for the stability and performance of these materials under different temperature conditions.

Differential scanning calorimetry (DSC)

Table 12. Results of DSC analysis of LDPE–starch–(EMA–Na)–1% ferric oxide blend

Sample	T _m (°C)	ΔH _f (J/g)	T _c (°C)	ΔH _c (J/g)	% crystallinity
LDPE	110	67	96	79	23.4
LDS–Na(1)Fe	110.86	51.41	98.83	57.26	17.9
LDS–Na(1)Fe(ab)	110.57	46.08	93.01	58.31	16.1

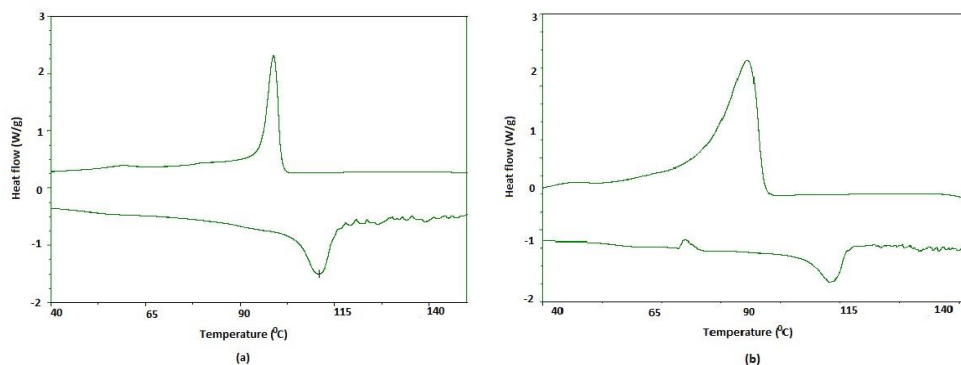


Figure 9. DSC curves of LDPE–starch–(EMA–Na)–1% ferric oxide blend: a) before biodegradation and b) after biodegradation

Table 12 along with Figure 9 provide insights into the thermal behavior of LDPE–starch–(EMA–Na) ferric oxide (74/20/5/1) blends both before and after undergoing biodegradation. These elements

contribute to understanding how the presence of ferric oxide impacts the thermal properties of the blends and how these properties change as a result of biodegradation.

The data in the table reveal that the addition of ferric oxide does not have any significant effect on the melting temperature (T_m) of pure LDPE. This suggests that the presence of ferric oxide does not alter the overall crystalline structure of LDPE, at least in terms of its melting behavior. The melting temperature is a key indicator of the crystalline arrangement of a polymer.

For the LDPE–starch–(EMA–Na)–ferric oxide blend, the incorporation of ferric oxide leads to a reduction in the crystallinity of LDPE. This decrease in crystallinity is likely related to the presence of an amorphous phase in the blend. The amorphous phase lacks the well–defined, ordered structure of the crystalline phase. This reduction in crystallinity could be significant because it may have contributed to the biodegradation process.

The decrease in crystallinity observed after two months of biodegradation is likely connected to the changes occurring during degradation, particularly in the amorphous phase of the polymer. Amorphous regions are generally more susceptible to degradation due to the lack of a highly ordered structure that provides stability.

The early alterations associated with degradation tend to manifest in the amorphous phase of the polymer first. As a result, the decrease in crystallinity observed could be indicative of changes taking place within the amorphous regions as a consequence of biodegradation. 3.11 Morphological studies

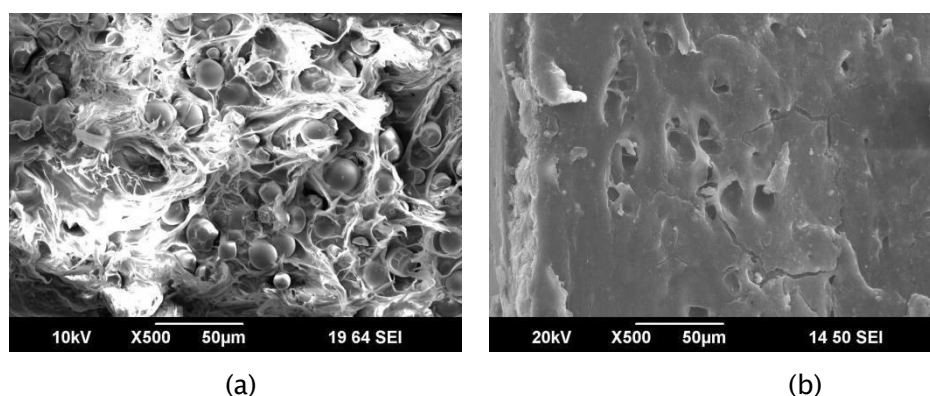


Figure 10. Scanning electron micrographs of LDPE–starch–(EMA–Na) (75/20/5) blend containing 1% Fe_2O_3 as pro–oxidant: (a) before biodegradation and (b) after biodegradation for two months

Figure 10 in the study displays scanning electron micrographs showcasing the cracked surfaces of an LDPE–starch–(EMA–Na) blend that incorporates 1% ferric oxide. The micrographs depict the material before and after undergoing two months of biodegradation in a culture medium. These images provide visual evidence of how the presence of ferric oxide and the biodegradation process impact the surface morphology of the blend (Saeed, 2022).

After the two–month biodegradation period, the micrographs reveal the presence of numerous tiny cavities on the LDPE–starch–(EMA–Na)–ferric oxide blend surface. This observation indicates that microorganisms have effectively eliminated starch from the blend. The presence of cavities is a result of the microbial action on the starch component. Interestingly, in the case of the ferric oxide–incorporated blend, the number of cavities is fewer compared to the LDPE–starch blend (depicted in Figure 11). This suggests that the inclusion of ferric oxide has some impact on limiting the extent of starch removal by microorganisms.

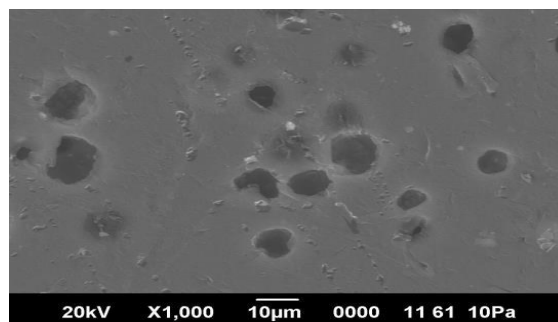


Figure 11. Scanning electron photo-micrograph of LDPE–starch blend after biodegradation in culture medium for eight weeks

The improved preservation of starch in the ferric oxide-incorporated blend might be due to the interaction between ferric oxide and the polymer matrix. This interaction could potentially hinder microbial access to the starch, slowing down its degradation. Additionally, the presence of the compatibilizer (EMA–Na) appears to play a role in enhancing the interfacial adhesion of the blend samples containing ionomer. This improvement in interfacial adhesion could contribute to the better preservation of the material's structure and components during biodegradation. The varying degrees of cavity formation and surface deterioration illustrate the complex interactions between the blend components, the biodegradation process, and the influence of additives like ferric oxide.

Conclusion

The incorporation of modest amounts of metal oxides (ferric oxide, manganese dioxide, titanium dioxide (rutile and anatase grades)) in EMA–Na compatible LDPE–starch blends resulted in minor modifications in LDPE mechanical properties. The addition of tiny amounts of titanium dioxide (rutile and anatase grades) resulted in a minor change in the melt flow index of LDPE. However, the addition of trace amounts of ferric oxide and manganese dioxide increased the melt flow index of LDPE. The tensile strength of all samples decreased significantly following immersion in the culture medium, demonstrating biodegradation of the blends by microorganisms, as validated by IR spectroscopy.

When exposed to UV radiation, the presence of trace amounts of metal oxides caused degradation of LDPE–starch–(EMA–Na) blends. After photobiodegradation, all of the samples showed a considerable drop in tensile strength and weight. The addition of metal oxides increased the rate of deterioration in the following order: $\text{Fe}_2\text{O}_3 > \text{MnO}_2 > \text{Ru} > \text{An}$. The addition of tiny amounts of metal oxides raised the storage modulus in all of the samples, indicating stiffening. The addition of modest amounts of metal oxides affects LDPE's thermal stability and crystallinity. The biodegradation of the pro-oxidant-incorporated blend samples is confirmed by SEM micrographs.

CRedit authorship contribution statement: Author 1: Methodology, Investigation, Formal Analysis Author 2: Review, proof reading Author 3: Supervision.

Declaration of competing interest: The authors declare that we have no known competing financial interests or personal relationships that could have appeared to influence the work reported in this paper.

References

1. Ammala, A., Bateman, S., Dean, K., Petinakis, E., Sangwan, P., Wong, S., ... Leong, K. H. (2011). An overview of degradable and biodegradable polyolefins. *Progress in Polymer Science*, 36(8), 1015–1049. doi:10.1016/j.progpolymsci.2010.12.002
2. Arkatkar, A., Arutchelvi, J., Sudhakar, M., Bhaduri, S., Uppara, P. V., & Doble, M. (2009). Approaches to enhance the biodegradation of polyolefins. *The Open Environmental Engineering Journal*, 2(1), 68–80. doi:10.2174/1874829500902010068

3. Bardají, D., & Moretto, J. (2020). João Pedro Rueda Furlan & Eliana Guedes Stehling ; A mini-review: current advances in polyethylene biodegradation.
4. Bulatović, V. O., Mandić, V., Kučić Grgić, D., & Ivančić, A. (2021). Biodegradable polymer blends based on thermoplastic starch. *Journal of Polymers and the Environment*, 29(2), 492–508. doi:10.1007/s10924-020-01874-w
5. Burelo, M., Hernández-Varela, J. D., Medina, D. I., & Treviño-Quintanilla, C. D. (2023). Recent developments in bio-based polyethylene: Degradation studies, waste management and recycling. *Heliyon*, 9(11), e21374. doi:10.1016/j.heliyon.2023.e21374
6. Burjupati, N. R., Kandiban, R., & Parthasarathy, A. (2020). Role of metal oxide nano particles in improving electrical, dielectric and thermal properties of polyethylene nano dielectric. In *Lecture Notes in Electrical Engineering* (pp. 182–193). Cham: Springer International Publishing.
7. Czigany, T., & Ronkay, F. (2021). Plastics in the shadow of the coronavirus: Don't prohibit, teach instead! *EXPRESS Polymer Letters*, 15(6), 490–491. doi:10.3144/expresspolymlett.2021.41
8. Deepika, S., & Jaya, M. R. (2015). Biodegradation of low density polyethylene by microorganisms from garbage soil. *J Exp Biol Agric Sci*, 3, 1–5.
9. Estrada-Monje, A., Alonso-Romero, S., Zitzumbo-Guzmán, R., Estrada-Moreno, I. A., & ZaragozaContreras, E. A. (2021). Thermoplastic starch-based blends with improved thermal and thermomechanical properties. *Polymers*, 13(23), 4263. doi:10.3390/polym13234263
10. Ferreira, F. G. D., Lima, M. A. G. A., Almeida, Y. M. B., & Vinhas, G. M. (2009). Evaluation of photodegradation in LDPE/modified starch blends. *Polímeros*, 19(4), 313–317. doi:10.1590/s0104-14282009000400011
11. Gemeinhardt, G. C., Moore, A. A., & Moore, R. B. (2004). Influence of ionomeric compatibilizers on the morphology and properties of amorphous polyester/polyamide blends. *Polymer Engineering & Science*, 44(9), 1721–1731. doi:10.1002/pen.20173
12. Guo, X., Wang, J., Kumar, S. G., & Rao, K. K. (2015). Zinc oxide based photocatalysis: tailoring surface-bulk structure and related interfacial charge carrier dynamics for better environmental applications. *Marine Pollution Bulletin*, 142(5), 3306–3351.
13. Inceoglu, F., & Menciloglu, Y. Z. (2013). Transparent low-density polyethylene/starch nanocomposite films. *Journal of Applied Polymer Science*, 129(4), 1907–1914. doi:10.1002/app.38811
14. Jakubowicz, I., Raheem, A., Aremo, B., & Adeoye, M. O. (2003). A Starch-Based Biodegradable Polyethylene for Municipal Solid Waste Mitigation. *Materials Sciences and Applications*, 80(1), 26–36.
15. Jiang, T., Duan, Q., Zhu, J., Liu, H., & Yu, L. (2020). Starch-based biodegradable materials: Challenges and opportunities. *Advanced Industrial and Engineering Polymer Research*, 3(1), 8–18. doi:10.1016/j.aiepr.2019.11.003
16. Jose, S., Aprem, A. S., Francis, B., Chandy, M. C., Werner, P., Alstaedt, V., & Thomas, S. (2004). Phase morphology, crystallisation behaviour and mechanical properties of isotactic polypropylene/high density polyethylene blends. *European Polymer Journal*, 40(9), 2105–2115. doi:10.1016/j.eurpolymj.2004.02.026
17. Ju, L., Mondschein, R. J., Vandenbrande, J. A., Arrington, C. B., Long, T. E., & Moore, R. B. (2020). Phosphonated Poly (ethylene terephthalate) ionomers as compatibilizers in extruded Poly (ethylene terephthalate)/Poly (m-xylylene adipamide) blends and oriented films. *Polymer*.
18. Kfoury, G., Raquez, J. M., Hassouna, F., Odent, J., Toniazzo, V., Ruch, D., & Dubois, P. (2013). Recent advances in high performance poly (lactide): from “green” plasticization to supertough materials via (reactive) compounding. *Frontiers in Chemistry*, 1.

21. Kushwaha, A., Goswami, L., Singhvi, M., & Kim, B. S. (2023). Biodegradation of poly(ethylene terephthalate): Mechanistic insights, advances, and future innovative strategies. *Chemical Engineering Journal* (Lausanne, Switzerland: 1996), 457(141230), 141230. doi:10.1016/j.cej.2022.141230
22. Mahieu, A., Terri , C., & Youssef, B. (2015). Thermoplastic starch films and thermoplastic starch/polycaprolactone blends with oxygen-scavenging properties: Influence of water content. *Industrial Crops and Products*, 72, 192–199. doi:10.1016/j.indcrop.2014.11.037
23. Maziad, N. A., Abdel Ghaffar, A. M., & Ali, H. E. (2021). Polyethylene film modification using polylactic acid - Starch additives and study ionizing radiation effect onto aging properties. *Environmental Progress & Sustainable Energy*, 40(2). doi:10.1002/ep.13556
24. Mural, P. K. S., Banerjee, A., Rana, M. S., Shukla, A., Padmanabhan, B., Bhadra, S., ... Bose, S. (2014). Polyolefin based antibacterial membranes derived from PE/PEO blends compatibilized with amine terminated graphene oxide and maleated PE. *Journal of Materials Chemistry. A, Materials for Energy and Sustainability*, 2(41), 17635–17648. doi:10.1039/c4ta03997a
25. Nakamura, E. M., Cordi, L., Almeida, G. S. G., Duran, N., & Mei, L. H. I. (2005). Study and development of LDPE/starch partially biodegradable compounds. *Journal of Materials Processing Technology*, 162–163, 236–241. doi:10.1016/j.jmatprotec.2005.02.007
27. Nofar, M., Sacligil, D., Carreau, P. J., Kamal, M. R., & Heuzey, M.-C. (2019). Poly (lactic acid) blends: Processing, properties and applications. *International Journal of Biological Macromolecules*, 125, 307–360. doi:10.1016/j.ijbiomac.2018.12.002
28. Ohtake, T., Ohtake, S., Kobayashi, H., Itoh, M., Asabe, N., Yabuki, K., & Murakami, O. (1995). Development of biodegradable LDPE compound and evaluation of its biodegradability. *Int Polym Sci Technol*, 22(2), 49–56.
29. Oner, B., & Gokkurt, T. (2019). Ayse Aytac: Studies on compatibilization of recycled polyethylene/thermoplastic starch blends by using different compatibilizer. *Open Chemistry*, 17, 557–563.
30. Oromiehie, A. R., Lari, T. T., & Rabiee, A. (2013). Physical and thermal mechanical properties of corn starch/LDPE composites. *Journal of Applied Polymer Science*, 127(2), 1128–1134. doi:10.1002/app.37877
31. Peter, Z., Kenyo, C., Renner, K., Krohnke, C., & Pukanszky, B. (2014). Decreased oxygen permeability of EVOH through molecular interactions. *EXPRESS Polymer Letters*, 8(10), 756– 766. doi:10.3144/expresspolymlett.2014.78
32. Queiroz, A. U., Collares-Queiroz, F. P., Ahmad, A. N., Lim, S. A., Navaranjan, N., Hsu, Y. I., & Uyama, H. (2009). Green sago starch nanoparticles as reinforcing material for green composites. *Journal of Macromolecular Science[®], Part C: Polymer Reviews*, 49(2).
33. Rhim, J.-W., Park, H.-M., & Ha, C.-S. (2013). Bio-nanocomposites for food packaging applications. *Progress in Polymer Science*, 38(10–11), 1629–1652. doi:10.1016/j.progpolymsci.2013.05.008
34. Rosa, D. S., Grillo, D., Bardi, M. A. G., Calil, M. R., Guedes, C. G. F., Ramires, E. C., & Frollini, E. (2009). Mechanical, thermal and morphological characterization of polypropylene/biodegradable polyester blends with additives. *Polymer Testing*, 28(8), 836– 842. doi:10.1016/j.polymertesting.2009.07.006
36. Roy, P. K., Surekha, P., Raman, R., & Rajagopal, C. (2009). Investigating the role of metal oxidation state on the degradation behaviour of LDPE. *Polymer Degradation and Stability*, 94(7), 1033–1039. doi:10.1016/j.polymdegradstab.2009.04.025

38. Sabetzadeh, M., Bagheri, R., & Masoomi, M. (2016). Effect of nanoclay on the properties of low density polyethylene/linear low density polyethylene/thermoplastic starch blend films. *Carbohydrate Polymers*, 141, 75–81. doi:10.1016/j.carbpol.2015.12.057
39. Saeed, S., Iqbal, A., & Deeba, F. (2022). Biodegradation study of Polyethylene and PVC using naturally occurring plastic degrading microbes. *Archives of Microbiology*, 204(8), 497. doi:10.1007/s00203-022-03081-8
40. Sanniyasi, E., Gopal, R. K., Gunasekar, D. K., & Raj, P. P. (2021). Biodegradation of low-density polyethylene (LDPE) sheet by microalga, *Uronema africanum* Borge. *Scientific Reports*, 11(1). doi:10.1038/s41598-021-96315-6
41. Steinmetz, Z., Wollmann, C., Schaefer, M., Buchmann, C., David, J., Tröger, J., ... Schaumann, G. E. (2016). Plastic mulching in agriculture. Trading short-term agronomic benefits for long-term soil degradation? *The Science of the Total Environment*, 550, 690–705. doi:10.1016/j.scitotenv.2016.01.153
42. Vinhas, G. M., de Lima, S. M., & Santos, L. A. (Eds.). (2007). Evaluation of the types of starch for preparation of LDPE/starch blends. *Agriculture, Agribusi Biotechnol*, 50(3).
43. Watanabe, T. (2010). Identification of fungi in Pictorial atlas of soil and seed fungi: morphologies of cultured fungi and key to species. CRC Press, 3.
44. Wilpiszewska, K., & Spychaj, T. (2011). Ionic liquids: Media for starch dissolution, plasticization and modification. *Carbohydrate Polymers*, 86(2), 424–428. doi:10.1016/j.carbpol.2011.06.001
45. Zhang, L., Brostowitz, N. R., Cavicchi, K. A., & Weiss, R. A. (2014). Perspective: Ionomer research and applications: Perspective: Ionomer research and applications. *Macromolecular Reaction Engineering*, 8(2), 81–99. doi:10.1002/mren.201300181
47. Zhang, Y., & Pedersen, J. N. (2022). Zheng Guo; Biodegradation of polyethylene and polystyrene: From microbial deterioration to enzyme discovery. *Biotechnology Advances*.